PROBLEMY MECHATRONIKI
UZBROJENIE, LOTNICTWO, INŻYNIERIA BEZPIECZEŃSTWA

ISSN 2081-5891

12, 1 (43), 2021, 59-74

PROBLEMS OF MECHATRONICS
ARMAMENT, AVIATION, SAFETY ENGINEERING

Preliminary Physical and Mathematical Model of the Recoil Operated Firearm within the Bolt Recoil Period

Damian SZUPIEŃKO*, Ryszard B. WOŹNIAK

Military University of Technology,
Faculty of Mechatronics, Armament and Aerospace, Institute of Armament Technology
2 Sylwestra Kaliskiego Str., 00-908 Warsaw, Poland
**Corresponding author's e-mail address and ORCID*:
damian.szupienko@wat.edu.pl; https://orcid.org/0000-0003-0202-9213

Received by the editorial staff on 10 September 2020
The reviewed and verified version was received on 22 February 2021

DOI 10.5604/01.3001.0014.7851

Abstract. This paper presents a preliminary physical and mathematical model which describes the specific action of an automatic, short recoil operated firearm with an accelerator. The model includes the characteristic stages of the automatic action for a short recoil operated firearm (during one half of a single shot cycle), which enables simulation and assessment of the effect of the firearm's system design parameters on the recoil velocities in specific recoil assembly components.
Keywords: firearms, small arms, firearm construction, mechanical engineering, internal ballistics

Nomenclature:

b – constant for Brawin's formula;
d – calibre;
F_{sl} – compression resistance force of the barrel assembly recoil spring;
F_{sz} – compression resistance force of the bolt assembly recoil spring;
i_p – kinematic ratio between the barrel assembly and the bolt assembly (or the accelerator transmission);
i_p' – derivative of kinematic ratio between the barrel assembly and the bolt assembly relative to the barrel assembly displacement;
k_{sl} – stiffness of the barrel assembly recoil spring;
k_{sz} – stiffness of the bolt assembly recoil spring;
l_w – overall projectile travel inside the barrel;
L_1, L_2 – recoil travel of the recoiling assembly in stage I and II;
L_{l1}, L_{l2}, L_{l3} – recoil travel of the barrel assembly in stage I, II, and III;
L_{z1}, L_{z2}, L_{z3}, L_{z4} – recoil travel of the bolt assembly in stage I, II, III, and IV;
m_{zo} – mass of recoiling assembly;
m_l – mass of barrel assembly;
m_z – mass of bolt assembly;
N_x – force of rifling resistance;
p – gas pressure in the barrel bore;
p_w – gas pressure at the projectile's exit from the barrel;
p_m – maximum gas pressure in the barrel bore;
p_{pw} – gas pressure at the post-muzzle stage end;
P_z – gas pressure force applied to the bolt face;
P_p – gas pressure force applied to the bottom part of the projectile;
Q_l – barrel assembly force of action on the bolt assembly translated by the accelerator;
Q_z – bolt assembly force of action on the barrel assembly translated by the accelerator;
Q_1, Q_2 – recoil initiation force of the recoiling assembly in stage I and II;
Q_{l3}, Q_{l4} – recoil initiation force of the barrel assembly in stage III and IV;
Q_{z3}, Q_{z4} – recoil initiation force of the bolt assembly in stage III and IV;
s – barrel bore cross-sectional surface area;
t_{op} – time in post-muzzle stage;
W_1, W_2 – recoil velocity of the recoiling assembly in stage I and II;
W_{l1}, W_{l2}, W_{l3} – recoil velocity of the barrel assembly in stage I, II, and III;
W_{z1}, W_{z2}, W_{z3}, W_{z4} – recoil velocity of the bolt assembly in stage I, II, III, and IV;
V_w – muzzle velocity of the projectile;
x_{0l} – pre-deflection of the barrel assembly recoil spring;
x_{0z} – pre-deflection of the bolt assembly recoil spring;
α_b – rifling angle;
β – coefficient of post-muzzle gas effect;
λ_p – projectile type coefficient [1];

μ_p – projectile-to-rifling friction factor;
ω – mass of propellant.

1. INTRODUCTION

Recoil operation (RO) was one the first fully effective operating actions for automatic firearms, and originates from the end of the 1890s. Despite the passing of time and extreme advancements in barrel firearm design, due to its advantages (listed in [2]) the RO remains very popular in automatic firearm designs made in Poland and abroad [3].

In RO firearms, the automatic action is driven by the force of recoil generated by the pressure of propellant gas, which acts on the bolt face. Length of travel of the recoiling assembly is a way of discriminating between short recoil operated (SRO) and long recoil operated (LRO) firearms. SRO firearms can be classified into solutions having additional features which assist proper automatic action, like accelerators of various types and muzzle boosters [2]. This paper presents a physical model and a preliminary mathematical model of a SRO firearm complete with a cam-lever accelerator. This design was chosen because it was easy to adapt the model both to SRO and LRO actions (where the conversion to long recoil operated action would be done by skipping the step with the accelerator's action and modifying the length of travel of the system's components).

2. PRELIMINARY PHYSICAL AND MATHEMATICAL MODEL OF SHORT RECOIL OPERATED FIREARM WITH ACCELERATOR

The preliminary physical model of a SRO firearm with an accelerator (Fig. 1) is based on the design of the Browning M2HB 12.7 mm calibre heavy machine gun [4], one of the most popular firearms of this type in the world [2].

The developed mathematical model describes the system action during one half of a single shot cycle. There are the following characteristic stages discriminated in the mathematical model of the system action during one half of a single shot cycle:

Stage I – from the start of the projectile's movement to when the projectile clears the barrel;
Stage II – from when the projectile clears the barrel to the start of the accelerator's action;
Stage III – from the start to the end of the accelerator's action;
Stage IV – from the end of the accelerator's action to when the bolt assembly reaches its rearward limit position.

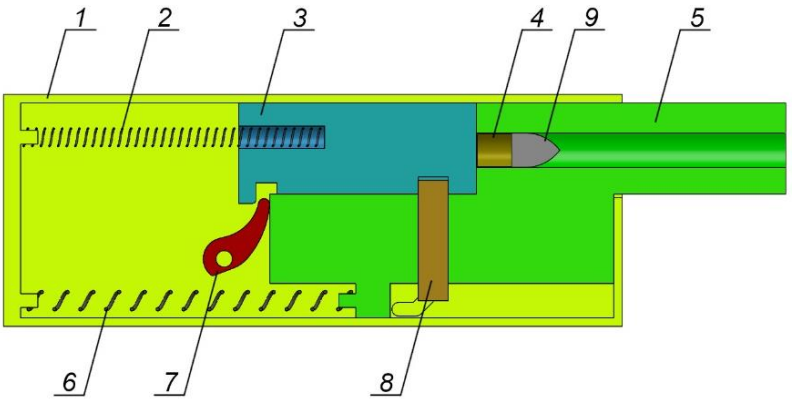

Fig. 1. Structural diagram of the SRO firearm with an accelerator: 1 – receiver; 2 – bolt assembly recoil spring; 3 – bolt assembly; 4 – case; 5 – barrel assembly; 6 – barrel assembly recoil spring; 7 – accelerator; 8 – breech lock; 9 – projectile

A method of analysis of the automatic firearm action similar to the one adopted for this physical and mathematical model is discussed in [5-9]. Given that the models are preliminary, their design ignores the friction between the components and the belt feed assembly used in the M2HB machine gun.

2.1. Stage I: Projectile motion in the barrel

During stage I, which extends from the start of motion of the projectile inside of the barrel and ends when the projectile clears the barrel, the recoiling assembly (which comprises the barrel assembly locked together with the bolt assembly) is under the impact of the gas pressure applied to the bolt face (gas pressure is applied to the bottom of the case, which acts on the bolt face) and the opposing forces which follow: the force of rifling resistance and the resistance forces of the barrel and bolt recoil springs (Fig. 2). Stage I is when the bolt assembly begins to be unlocked by the dropping breech lock (Fig. 2, #8).

The recoil force Q_1 of the recoiling assembly with mass $m_{zo}=m_z+m_l$ in stage I (1):

$$Q_1 = P_z - F_{sz} - F_{sl} - N_x \tag{1}$$

Gas pressure force P_z applied to the bolt face with surface area s:

$$P_z = p \cdot s \tag{2}$$

Force of rifling resistance N_x [9]:

$$N_x = \lambda_p \cdot \left(\mu_p \cdot tg\alpha_b + tg^2\alpha_b\right) \cdot p \cdot s \tag{3}$$

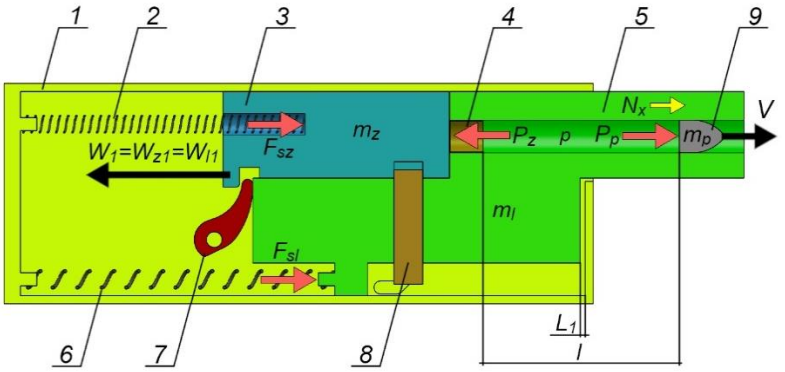

Fig. 2. Physical model of the analysed system in stage I: 1 – receiver; 2 – bolt assembly recoil spring; 3 – bolt assembly; 4 – case; 5 – barrel assembly; 6 – barrel assembly recoil spring; 7 – accelerator; 8 – breech lock; 9 – projectile

The resistance forces of the barrel and bolt assembly recoil springs are expressed as:

$$F_{sz} = k_{sz} \cdot (x_{0z} + L_1) \tag{4}$$

and

$$F_{sl} = k_{sl} \cdot (x_{0l} + L_1) \tag{5}$$

The equation of the recoil assembly motion in stage I is expressed as:

$$m_{zo} \cdot \frac{dW_1}{dt} = \left[1 - \lambda_p \cdot \left(\mu_p \cdot tg\alpha + tg^2\alpha\right)\right] \cdot p \cdot s - k_{sz} \cdot (x_{0z} + L_1) + \\ -k_{sl} \cdot (x_{0l} + L_1) \tag{6}$$

The recoiling assembly acceleration in stage I:

$$\frac{dW_1}{dt} = \frac{s}{m_{zo}} \cdot \left[1 - \lambda_p \cdot \left(\mu_p \cdot tg\alpha + tg^2\alpha\right)\right] \cdot p - \frac{k_{sz}}{m_{zo}} \cdot (x_{0z} + L_1) + \\ -\frac{k_{sl}}{m_{zo}} \cdot (x_{0l} + L_1) \tag{7}$$

Definition of the linear velocity of the recoiling assembly in stage I:

$$\frac{dL_1}{dt} = W_1 \tag{8}$$

2.2. Stage II: From when the projectile clears the barrel to the start of the accelerator's action

In stage II, the recoiling assembly is under the effect of the gas pressure in the barrel bore and the opposing resistance forces of the barrel and bolt assembly recoil springs (Fig. 3). When stage II is complete, the bolt assembly is fully unlocked and the accelerator's action begins.

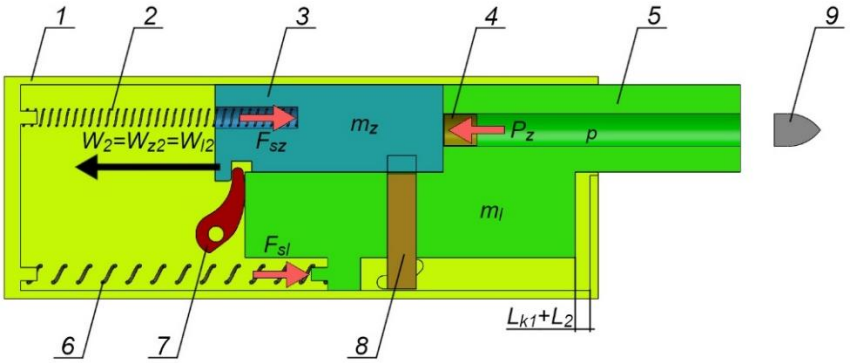

Fig. 3. Physical model of the analysed system during second stage of operation: 1 – receiver, 2 – bolt assembly recoil spring, 3 – bolt assembly, 4 – cartridge case, 5 – barrel assembly, 6 – barrel assembly recoil spring, 7 – accelerator, 8 – breech lock, 9 – projectile

The recoil force of the recoiling assembly in stage II, Q_2, is expressed as follows:

$$Q_2 = P_z - F_{sz} - F_{sl} \tag{9}$$

The post-muzzle gas pressure is expressed as follows, according to Brawin's empirical formula [10]:

$$p = p_w \cdot e^{-\frac{t_{op}}{b}} \tag{10}$$

Constant b introduced to relationship (10) is expressed as relationship [10]:

$$b = \frac{(\beta - 0{,}5) \cdot \omega}{s \cdot (p_w - p_{pw})} \cdot v_w \tag{11}$$

The coefficient of post-muzzle gas effect value β present in relationship (11) is expressed with empirical formula [10]:

$$\beta = 1{,}5 + \frac{6{,}45}{\left(\frac{p_m}{p_w} \cdot \frac{l_w}{d}\right) \cdot 0{,}23} \tag{12}$$

Similar to stage I, the equation of the recoiling assembly motion in stage II is expressed as:

$$m_{zo} \cdot \frac{dW_2}{dt} = p \cdot s - k_{sz} \cdot (x_{0z}+L_2) - k_{sl} \cdot (x_{0l} + L_2) \tag{13}$$

The recoiling assembly acceleration in stage II:

$$\frac{dW_2}{dt} = \frac{s}{m_{zo}} \cdot p - \frac{k_{sz}}{m_{zo}} \cdot (x_{0z} + L_2) - \frac{k_{sl}}{m_{zo}} \cdot (x_{0l} + L_2) \tag{14}$$

The relationship which expresses the definition of recoiling assembly linear velocity in stage II remains unchanged from stage I (8).

2.3. Stage III: Accelerator's action

In stage III, the barrel assembly is separated from the bolt assembly. The barrel assembly in motion is under the effect of the resistance force of the barrel assembly recoil spring and the force of action of the bolt assembly translated by the accelerator.

This is similar to what happens with the bolt assembly, which is under the effect of the gas pressure, the resistance force of the recoil spring, and the force of action of the barrel assembly translated by the accelerator (Fig. 4).

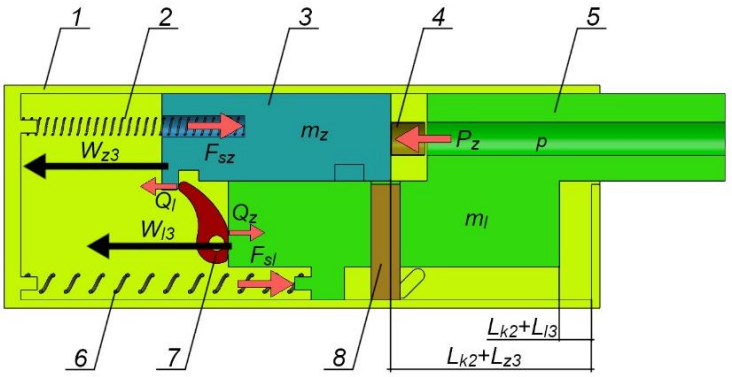

Fig. 4. Physical model of the analysed system during third stage of operation: 1 – receiver, 2 – bolt assembly recoil spring, 3 – bolt assembly, 4 – cartridge case, 5 – barrel assembly, 6 – barrel assembly recoil spring, 7 – accelerator, 8 – breech lock

The motive force of the barrel in stage III, Q_{l3}, is expressed as follows:

$$Q_{l3} = -F_{sl} - Q_z \tag{15}$$

The motive force of the bolt in stage III, Q_{z3}, is expressed as follows:

$$Q_{z3} = -F_{sz} + Q_l \tag{16}$$

Hence, the equations of motion of the barrel (the primary link) and the bolt (the mating link) are expressed, respectively, as:

$$m_l \cdot \frac{dW_{l3}}{dt} = -k_{sl} \cdot (x_{0l} + L_{l3}) - Q_z \tag{17}$$

$$m_z \cdot \frac{dW_{z3}}{dt} = -k_{sz} \cdot (x_{0z} + L_{z3}) + Q_l + p \cdot s \tag{18}$$

The relationship between internal forces, Q_z and Q_l acting on the primary link and the mating link (and without the forces of friction in the system in this preliminary model) is expressed as [11]:

$$Q_z = i_p \cdot Q_l \tag{19}$$

The accelerator's kinematic ratio, i_p is the ratio of the mating link displacement, dL_{z3} (or the displacement of the bolt) and the primary link displacement, dL_{l3} (or the displacement of the barrel) along the travel of the barrel assembly along which the accelerator acts [11]:

$$i_p = \frac{dL_{z3}}{dL_{l3}} \tag{20}$$

Equation (17) can be expressed as:

$$m_l \cdot \frac{dW_{l3}}{dt} = -k_{sl} \cdot (x_{0l} + L_{l3}) - i_p \cdot Q_l \tag{21}$$

When force Q_l is determined with equation (18) and substituted in equation (21), the result is equation:

$$\begin{aligned} m_l \cdot \frac{dW_{l3}}{dt} &= -k_{sl} \cdot (x_{0l} + L_{l3}) + \\ -i_p \cdot \left[m_z \cdot \frac{dW_{z3}}{dt} + k_{sz} \cdot (x_{0z} + L_{z3}) - p \cdot s \right] & \end{aligned} \tag{22}$$

The relationship which expresses the motion of the mating link relative to the primary link is [11]:

$$\frac{dW_{z3}}{dt} = i_p \cdot \frac{dW_{l3}}{dt} + i_p' \cdot \left(\frac{dL_{l3}}{dt} \right)^2 \tag{23}$$

When equation (23) is substituted to equation (22) and the equation is rearranged, the result is the equation of two-link mechanism motion as:

$$\begin{aligned} \left(m_l + i_p^2 \cdot m_z \right) \cdot \frac{dW_{l3}}{dt} + i_p \cdot i_p' \cdot m_z \cdot \left(\frac{dL_{l3}}{dt} \right)^2 = \\ = -k_{sl} \cdot (x_{0l} + L_{l3}) - i_p \cdot k_{sz} \cdot (x_{0z} + L_{z3}) + i_p \cdot p \cdot s \end{aligned} \tag{24}$$

When the barrel acceleration is determined from equation (24), the result is equation:

$$\frac{dW_{l3}}{dt} = -\frac{k_{sl} \cdot (x_{0l} + L_{l3})}{m_l + i_p^2 \cdot m_z} - \frac{i_p \cdot k_{sz} \cdot (x_{0z} + L_{z3})}{m_l + i_p^2 \cdot m_z} + \\ - \frac{i_p \cdot i_p' \cdot m_z \cdot \left(\frac{dL_{l3}}{dt}\right)^2}{m_l + i_p^2 \cdot m_z} + \frac{i_p \cdot p \cdot s}{m_l + i_p^2 \cdot m_z} \tag{25}$$

A similar process of determination of the stage III bolt acceleration provides equation:

$$\frac{dW_{z3}}{dt} = -\frac{k_{sz} \cdot (x_{0z} + L_{z3})}{m_z + \frac{m_l}{i_p^2}} - \frac{k_{sl} \cdot (x_{0l} + L_{l3})}{i_p \cdot m_z + \frac{m_l}{i_p}} + \\ + \frac{m_l \cdot i_p' \cdot \left(\frac{dL_{l3}}{dt}\right)^2}{m_l + i_p^2 \cdot m_z} + \frac{p \cdot s}{m_z + \frac{m_l}{i_p^2}} \tag{26}$$

The relationships which express the definition of linear velocity of the bolt assembly and the barrel assembly in stage III will be analogical to the relationships in stage I and II.

2.4. Stage IV: Bolt motion by forces of inertia

In stage IV, the barrel assembly remains stationary, while the motion of the bolt assembly propelled by forces of inertia is opposed by the resistance force of the bolt assembly recoil spring (Fig. 5).

The force acting on the bolt assembly in stage IV is expressed as follows:

$$Q_{z4} = -F_{sz} \tag{27}$$

The equation of the bolt assembly motion in stage IV is expressed as follows:

$$m_z \cdot \frac{dW_{z4}}{dt} = -k_{sz} \cdot (x_{0z} + L_{z4}) \tag{28}$$

The bolt assembly acceleration in stage IV can be expressed as follows:

$$\frac{dW_{z4}}{dt} = -\frac{k_{sz}}{m_z} \cdot (x_{0z} + L_{z4}) \tag{29}$$

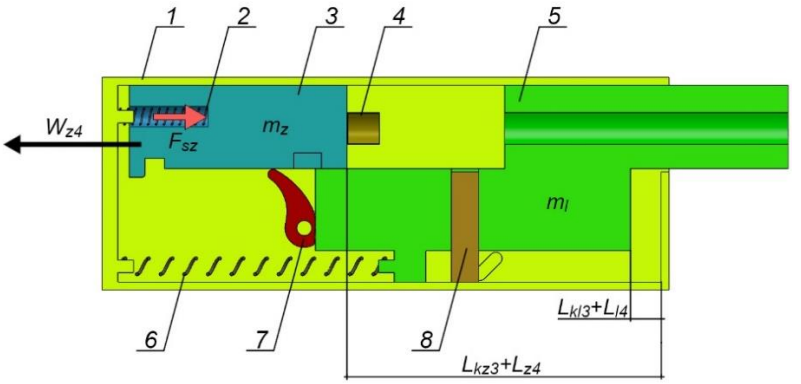

Fig. 5. Physical model of the analysed system during fourth stage of operation: 1 – receiver, 2 – bolt assembly recoil spring, 3 – bolt assembly, 4 – cartridge case, 5 – barrel assembly, 6 – barrel assembly recoil spring, 7 – accelerator, 8 – breech lock

The relationship which expresses the definition of bolt assembly linear velocity in stage IV remains unchanged from the previous stages.

3. RESULTS OF THE CALCULATIONS OF THE SYSTEM ACTION

The data inputs for the calculations driven by the model were acquired from testing the characteristics of the recoil springs of interest and the weight and dimensions of selected components of the Browning M2HB 12.7 mm calibre machine gun in the collection of the Institute of Armament Technology, Laboratory of Weapons and Ammunition at the Military University of Technology in Warsaw (Poland).

The weight of the components was measured with a WLC 60/120/C2/K precision scale, while the dimensions of the barrel extension and of the bolt (due to their straightforward construction) were measured with a digital calliper. The stiffness of the recoil springs of the M2HB machine gun and the pre-load force of the bolt recoil assembly (which comprises a guide rod and a pre-tensioned spring) were determined by compression testing with measurement of deflection and force on a Thümler Z3 strength tester.

Given that the guide rod was essential to prevent buckling of the bolt assembly recoil spring, the construction of the barrel recoil assembly, and the construction of the strength tester clamps, it was only possible to measure the characteristics in the deflection range of 0-75 mm (where the operating deflection of the bolt assembly recoil spring is 181 mm and the pre-deflection and operating deflection of the barrel assembly recoil spring is 63 mm and 28 mm, respectively). Given the resulting linear characteristics of the recoil springs of interest, the calculations for the entire deflection range of the recoil springs included the stiffness values determined in the deflection range of 0-75 mm.

To determine the dimensions and the ratio of the accelerator, its geometrical features were tested with a Starrett VB400 vertical bench top optical comparator. With the known dimensions of the accelerator and of the housing to which the barrel assembly return action is attached, it was possible to determine the ratio (20) for each successive position of the primary link (the barrel with its housing). The positioning process began with the mapping of geometrical features of the accelerator and parts of the barrel extension and of the bolt as three-dimensional solids in SolidWorks. The generated solids were arranged in a configuration which represented the layout of the respective components in the Browning M2HB machine gun. The ratios were determined by modifying the position of the barrel assembly within 19-28 mm (which is the travel of the barrel assembly in stage III of the system's action) in 0.25 mm increments and by measuring the displacement of the bolt assembly as an effect of the movement of the barrel assembly. The barrel displacement increment value was chosen to achieve a relatively stepless trend of the curve crossing the discrete values of ratio with the lowest possible number of points. When the accelerator starts acting, the barrel assembly and the bolt assembly move at the same velocity and the accelerator's ratio for $\Delta x_l=0$ is $i_p=1$.

The application of the determined ratio values in the mathematical model – considering the nature of the applied equations – required an expression of the ratio with an equation in the function of the barrel assembly displacement, Δx_l. The trend of the ratio function was approximated with a feature integrated in MATLAB which applies the least squares method (it is the function *polyfit*).

The degree of the polynomial which approximated the trend was increased until the fit accuracy factor reached the value R^2 = 0.999 (and ultimately, the accelerator's ratio was approximated with a 10th degree polynomial) (Fig. 6).

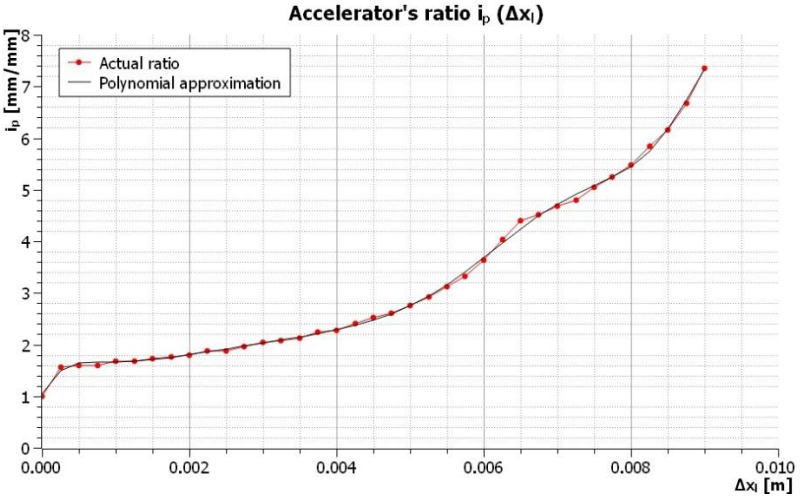

Fig. 6. Chart of the relationship between the accelerator's ratio and the barrel assembly travel during the acceleration stage

The trends of gas pressure values inside of the barrel bore were used with the barrel velocity of the projectile from a Browning 12.7 × 99 mm NATO round determined in [12] were used in the calculations. The data applied in the calculation of the system operation of interest is listed in Table 1.

The parameter values listed in Table 1 were input to calculate the operation of a SRO firearm with accelerator (Fig. 7).

Table 1. Values of simulation input parameters

Parameter	Designation	Value
Mass of propellant	ω_p [g]	16
Mass of projectile	m [g]	42.87
Barrel bore cross-sectional surface area	s [mm^2]	132.26
Barrel's firing chamber volume	W_0 [cm^3]	19
Overall projectile travel inside of the barrel	l_w [m]	1.068
Projectile-to-rifling friction factor	μ_p	0.16
Projectile type coefficient	λ_p	0.48
Rifling angle	α_b [°]	5.98
Recoil travel of the recoiling assembly until the start of the accelerator action	$L_{pprzysp}$ [m]	0.019
Recoil travel of the barrel assembly at the end of the accelerator action	$L_{kprzysp}$ [m]	0.028
Overall recoil travel of the bolt assembly	L_z [m]	0.181
Mass of bolt assembly	M_z [kg]	2.32
Mass of barrel assembly	M_l [kg]	13.8
Stiffness of the barrel assembly recoil spring	k_{sz} [N/mm]	2.74
Pre-deflection of the barrel assembly recoil spring	x_{0l} [m]	0.063
Stiffness of the bolt assembly recoil spring	k_{sz} [N/mm]	0.61
Pre-deflection of the bolt assembly recoil spring	x_{0z} [m]	0.0153
Coefficients of accelerator's ratio polynomial	a_{10}	$-4{,}347\cdot10^{24}$
	a_9	$1{,}894\cdot10^{23}$
	a_8	$-3{,}535\cdot10^{21}$
	a_7	$3{,}176\cdot10^{19}$
	a_6	$-2{,}435\cdot10^{17}$
	a_5	$1{,}038\cdot10^{15}$

Table 1. cont'd. Values of simulation input parameters

Parameter	Designation	Value
Coefficients of accelerator's ratio polynomial	a_4	$-2.896 \cdot 10^{12}$
	a_3	5129656764
	a_2	-5328134.025
	a_1	2892.447
	a_0	1.039
Heat of propellant combustion	q_s [MJ/kg]	5.15
Propellant force	f [MJ/kg]	1.0309
Propellant gas co-volume	α [dm^3/kg]	1
Propellant gas adiabatic exponent	k	1.2
Propellant density	δ_p [kg/m^3]	1590
Coefficient of linear burning rate	u_1 [m/(s·Pa)]	$0.71 \cdot 10^{-9}$
Initial surface area of propellant grain	S_1 [mm^2]	12.56
Initial volume of propellant grain	Λ_1 [mm^3]	2.87
Secondary work coefficient constant	K	1.1
Ignition pressure	p_z [MPa]	5
Bullet forcing pressure	p_0 [MPa]	30
Propellant grain coefficients of shape	χ	1.316
	λ	-0.24
	μ	0

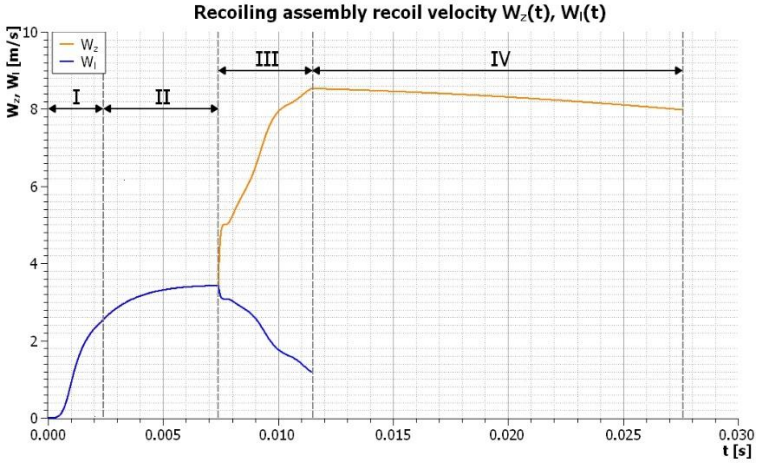

Fig. 7. Recoil velocity of the recoiling assembly with the characteristics stage of operation shown

The formulated mathematical model was used to develop a calculation routine in MATLAB. The equations were processed by Eulerian integration, given the preliminary character of the model and an easy implementation in MATLAB. The software calculation was run with an integration step of 0.1 μs.

For a preliminary verification of the correctness of 'action' of the mathematical model in the bolt acceleration stage, the calculated velocity values of the parts in the bolt acceleration stage (without the simultaneous action of the post-muzzle gas pressure on the bolt) were compared to the simulation results from the SolidWorks by application of the SolidWorks Motion module (Fig. 8).

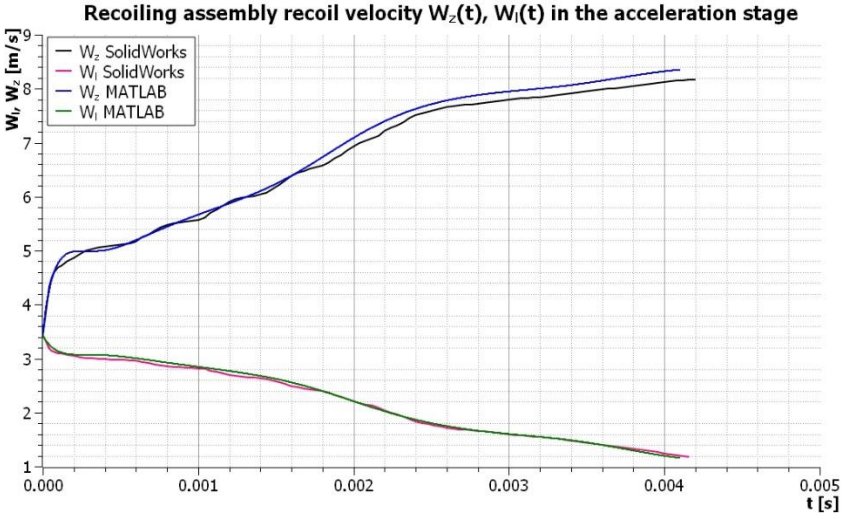

Fig. 8. Recoil velocity curves of the recoiling parts in stage III of operation determined as a result of SolidWorks motion analysis and the calculation using the mathematical model

4. CONCLUSIONS

1. For the case of interest, as a result of the calculations driven by the mathematical model, when the recoil assembly is separated the recoil velocity of that assembly was 3.43 m/s, the bolt velocity reached 8.35 m/s at the end of the acceleration stage, whereas the barrel assembly recoil velocity was 1.18 m/s.
2. The differences in the velocity of the recoiling parts during the bolt assembly acceleration stage and provided by the calculation driven by the mathematical model and as a result of the kinematic simulation in SolidWorks could result from the differences between the actual and the approximate ratio of the parts and the parameters used in the definition of contacts.

3. The motion equations applied in the mathematical model for the recoiling assembly parts in the acceleration stage only included the value of the kinematic ratio between the assembly parts, which allowed a relatively straightforward adaptation of the model to certain designs, like those with a single recoil assembly and the interrelation of the position of the barrel and bolt assemblies along the whole travel of the barrel recoil.
4. The developed preliminary mathematical model can be also applied in non-accelerated systems (like standard short recoil and long recoil systems), which can be done by omitting the bolt acceleration stage and modifying the length of recoil travel for the individual components.
5. A full proof of correct operation of the model will only be possible by experimental tests and comparison of the curve trends generated with them to the numerical simulation results.

ACKNOWLEDGEMENT AND FUNDING

The authors thank PhD Mirosław Zahor, PhD Jacek Kijewski and PhD Bartosz Fikus from the Military University of Technology (Warsaw, Poland) for providing technical and content-related comments.

The authors received no financial support for the research, authorship, and/or publication of this article.

REFERENCES

[1] Serebriakow M. 1955. *Balistyka wewnętrzna*. Warszawa: Wydawnictwo MON.
[2] Szupieńko Damian, Ryszard Woźniak, Mirosław Zahor. 2019. Analiza stanu techniki w dziedzinie automatycznej broni palnej działającej na zasadzie odrzutu lufy. Referat wygłoszony w ramach *VII Konferencji Młodych Naukowców Wiedza i Innowacje wiWAT 2019,* Nowy Dwór Mazowiecki, 3-5 grudnia 2019.
[3] Richard D. Jones. 2019. *Jane's Weapons: Infantry 2019-2020,* Coulsdon: Ihs Markit.
[4] *Training Circular No. 3-22.50 : Heavy Machine Gun M2 Series*. 2017. Waszyngton: US Army, Headquarters, Department of the Army.
[5] Surma Zbigniew, Stanisław Torecki, Ryszard Woźniak. 2005. „Model balistyczny układu miotającego z odprowadzeniem gazów prochowych", *Biuletyn WAT* LIV (11) : 43-56.
[6] Torecki Stanisław, Zbigniew Surma, Ryszard Woźniak. 2006. „Napęd suwadła broni automatycznej w powylotowym okresie strzału". *Biuletyn WAT* LV (3) : 297-309.

[7] Leśnik Grzegorz, Zbigniew Surma, Stanisław Torecki, Ryszard Woźniak. 2009. „Termodynamiczny model działania broni z odprowadzeniem gazów prochowych w okresie napędzania suwadła". *Biuletyn WAT* LVIII (3) : 193-209.
[8] Surma Zbigniew, Łukasz Szmit, Stanisław Torecki, Ryszard Woźniak. 2010. „Model matematyczny podrzutu broni działającej na zasadzie odprowadzenia gazów". *Problemy mechatroniki. Uzbrojenie, lotnictwo, inżynieria bezpieczeństwa – Problems of Mechatronics. Armament, Aviation, Safety Engineering* 1 (2) : 51-63.
[9] Surma Zbigniew, Łukasz Szmit, Stanisław Torecki, Ryszard Woźniak. 2011. „Niektóre wyniki badań symulacyjnych wpływu charakterystyk konstrukcyjnych karabinka automatycznego na jego odrzut i podrzut". *Problemy mechatroniki. Uzbrojenie, lotnictwo, inżynieria bezpieczeństwa - Problems of Mechatronics. Armament, Aviation, Safety Engineering* 2 (2) : 73-83.
[10] Szmit Łukasz. 2017. *Badania teoretyczne i doświadczalne odrzutu, podrzutu i obrotu automatycznej broni strzeleckiej.* Warszawa: Wydawnictwo WAT.
[11] Kafliński Z. 1981. *Lotnicza broń lufowa część II: Podstawy budowy urządzeń i mechanizmów broni.* Warszawa: Wydawnictwo WAT.
[12] Szupieńko Damian. 2019. *Projekt wstępny karabinu przeciwsprzętowego kalibru 12,7 mm.* Praca magisterska. Warszawa: Wydawnictwo WAT.

Wstępny model fizyczny i matematyczny działania broni z odrzutem lufy w okresie odrzutu zamka

Damian SZUPIEŃKO, Ryszard B. WOŹNIAK

Wojskowa Akademia Techniczna,
Wydział Mechatroniki, Uzbrojenia i Lotnictwa, Instytut Techniki Uzbrojenia
ul. gen. Sylwestra Kaliskiego 2, 00-908 Warszawa

Streszczenie. W pracy przedstawiono wstępny model fizyczny i matematyczny opisujący specyfikę pracy automatycznej broni palnej działającej na zasadzie krótkiego odrzutu lufy (KOL) z przyspieszaczem. Model ten uwzględnia okresy charakterystyczne działania automatyki broni z KOL (w trakcie połowy cyklu jednego strzału), umożliwiając przeprowadzenie symulacji pozwalających na ocenę wpływu parametrów konstrukcyjnych układu na prędkości odrzutu poszczególnych elementów zespołu odrzucanego.
Słowa kluczowe: broń palna, broń strzelecka, konstrukcja broni, mechanika, balistyka wewnętrzna